Partitioning Roles of Side Chains in Affinity, Orientation, and Catalysis with Structures for Mutant Complexes: Asparagine-229 in Thymidylate Synthase[†,‡]

Janet S. Finer-Moore,*[,§] Lu Liu,[||] Christian E. Schafmeister,[⊥] David L. Birdsall,[§] Ted Mau,[⊥] Daniel V. Santi,[§,||] and Robert M. Stroud[§]

Department of Biochemistry and Biophysics, Department of Pharmaceutical Chemistry, and Graduate Group in Biophysics, University of California, San Francisco, San Francisco, California 94143-0448

Received November 20, 1995; Revised Manuscript Received February 16, 1996[⊗]

ABSTRACT: Thymidylate synthase (TS) methylates only dUMP, not dCMP. The crystal structure of TS·dCMP shows dCMP 4-NH_2 excluded from the space between Asn-229 and His-199 by the hydrogen bonding and steric properties of Asn-229. Consequently, 6-C of dCMP is over 4 Å from the active site sulfhydryl. The Asn-229 side chain is prevented from flipping 180° to an orientation that could hydrogen bond to dCMP by a hydrogen bond network between conserved residues. Thus, the specific binding of dUMP by TS results from occlusion of competing substrates by steric and electronic effects of residues in the active site cavity. When Asn-229 is replaced by a cysteine, the Cys-229 Sγ rotates out of the active site, and the mutant enzyme binds both dCMP and dUMP tightly but does not methylate dCMP. Thus simply admitting dCMP into the dUMP binding site of TS is not sufficient for methylation of dCMP. Structures of nucleotide complexes of TS N229D provide a reasonable explanation for the preferential methylation of dCMP instead of dUMP by this mutant. In TS N229D·dCMP, Asp-229 forms hydrogen bonds to 3-N and 4-NH_2 of dCMP. Neither the Asp-229 carboxyl moiety nor ordered water appears to hydrogen bond to 4-O of dUMP. Hydrogen bonds to 4-O (or 4-NH_2) have been proposed to stabilize reaction intermediates. If their absence in TS N229D·dUMP persists in the ternary complex, it could explain the 10^4-fold decrease in k_{cat}/K_m for dUMP.

Mutation of key residues involved in binding reactants in transition states addresses the relative contributions of the residues both to enzymatic rate and to specific binding. Binding interactions of an enzyme with its biologically appropriate substrate rarely achieve the high affinity possible when the binding interactions are optimal. The binding of biotin by streptavidin is an example of binding that is closer to optimal, with $\Delta G_f \sim 21$ kcal/M and $K_d \sim 10^{-15}$ M (Chaiet & Wolf, 1964). There are several reasons for this. Enzymes evolve to operate on the correct substrate at physiological concentrations. The difference between the observed binding energy and that theoretically possible can be turned toward enhancing catalytic rate, as seen in the increase in k_{cat} with larger substrates in serine proteases, for example (Fersht, 1985). The enzyme binding site must also encode the lack of binding of other physiologically present molecules which would act as inhibitors or even as alternate substrates. This latter role is often overlooked in the search for a molecular basis for protein function. We probe this discriminatory role in mutants that alter preference in binding and catalysis.

In the dUMP-methylating enzyme thymidylate synthase (TS),[1] Asn-229 makes two hydrogen bonds to the pyrimidine ring of dUMP and to that of the product, dTMP. It is the only side chain that is hydrogen bonded to the dUMP pyrimidine base in ternary complexes of TS, and the hydrogen bond it donates to 4-O interacts directly with the enolate formed in the reaction mechanism. Its key role in providing a donor to 4-O and an acceptor for 3-NH of dUMP and its conservation among all known TS sequences suggest it encodes specificity of the enzyme for dUMP versus other nucleotides. Indeed, TS does not methylate dCMP and binds this nucleotide with a $K_d \sim$ 400-fold higher than that for dUMP (Liu & Santi, 1993a).

Mutating Asn-229 to smaller residues that no longer provide hydrogen bonds to the pyrimidine ring has little effect on K_d for dUMP, while several of these variants bind dCMP with a K_d comparable to that of dUMP in wild-type TS (Liu & Santi, 1993a). dCMP is not a substrate for any of these mutants. However, mutation of Asn-229 to aspartate yields a TS variant that specifically methylates dCMP (Hardy & Nalivaika, 1992; Liu & Santi, 1992).

To discover the structural basis for specific methylation of dUMP, and for the change in specificity that occurs when

[†] This work was supported by NIH Grants CA-41323 to J.S.F.-M. and R.M.S. and CA-14394 to D.V.S. C.E.S. and T.M. are supported by Howard Hughes Medical Institute predoctoral fellowships.

[‡] Coordinates for these structures are deposited in the Brookhaven Protein Data Bank. The access codes are 1NJA, 1NJB, 1NJC, 1NJD, and 1NJE.

[§] Department of Biochemistry and Biophysics.

[||] Department of Pharmaceutical Chemistry.

[⊥] Graduate Group in Biophysics.

[⊗] Abstract published in *Advance ACS Abstracts,* April 1, 1996.

[1] Abbreviations: TS, thymidylate synthase; dUMP, 2′-deoxyuridine 5′-monophosphate; dCMP, 2′-deoxycytidine 5′-monophosphate; dUrd, deoxyuridine; dCyd, deoxycytidine; CH_2-H_4folate, 5,10-methylene-5,6,7,8-tetrahydrofolate; F_o, measured structure factor amplitude; F_c, calculated structure factor amplitude; $(F_o - F_c)\alpha_{calc}$ map, electron density map calculated with coefficients $(|F_o| - |F_c|)$ and phases calculated from the coordinates; $(2F_o - F_c)\alpha_{calc}$ map, electron density map calculated with coefficients $(2|F_o| - |F_c|)$ and phases calculated from the coordinates.

0006-2960/96/0435-5125$12.00/0

Table 1: Crystallographic Statistics

mutant	cell axes (Å)	resoln (Å)	σ_{cutoff}	no. of obsd reflections	no. of unique reflections	% complete	$I/\sigma(I)$	R (%)
WT·dCMP	78.5, 242.4	2.3	1	39 357	14 073	67	5.0	10.0[a]
N229D·dUMP	78.4, 242.3	2.2	1	37 757	13 487	57	6.1	9.7[a]
N229D·dCMP	79.2, 229.6	2.5	0	41 508	14 050	89	6.7	10.4[a]
N229C·dUMP	78.7, 242.1	2.75	0	34 873	9 421	75	6.4	9.2[b]
N229C·dCMP	78.7, 230.6	2.2	0	45 354	17 232	76	7.6	8.4[a]

[a] $R_{merge} = \{[\sum_{hkl}\sum_i|I_{av} - I_i|]/\sum_{hkl}\sum_i I_i\} \times 100$. [b] $R_{sym} = \{\sum_{hkl}(\sum_i[(I_{av} - I_i)/\sigma(I_i)]^2/\sum_i[I_{av}/\sigma(I_i)]^2)\}^{1/2} \times 100$.

Asn-229 is mutated to an aspartate, we determine the crystal structures of dCMP and dUMP complexes with wild-type enzyme and with two mutants, TS N229C and TS N229D. Results show that Asn-229, Gln-217, Cys-198, and His-199 side chains together define a pocket for the base that admits a limited number of 3-N or 4-C substituents. Smaller side chains give more space for the base to bind, while aspartic acid restricts dUMP to a position slightly outside the normal binding pocket, much further from His-199. Consequently, it is possible to design an enzyme that specifically methylates alternate substrates (Costi et al., 1996, and unpublished results).

METHODS

Mutagenesis and Crystallization. TS N229D and TS N229C *Lactobacillus casei* TS were prepared by cassette mutagenesis of the synthetic TS gene pSCTS9 (Climie et al., 1990), expressed in *Escherichia coli* χ2913 (thy$^-$), and purified by sequential chromatography on phosphocellulose and hydroxylapatite (Kealey & Santi, 1992) as described (Liu & Santi, 1992). Hexagonal bipyramidal crystals were grown, generally as described in Hardy et al. (1987), by vapor diffusion from 6 μL drops containing 3.5−6.0 mg/mL protein and 2−20 mM dUMP or dCMP in 40 mM potassium phosphate (pH 7.0), 1 mM DTT, and 1−2% ammonium sulfate (percent saturated). Drops were suspended over just the phosphate buffer (40 mM phosphate at pH 7.0), DTT, and EDTA. Crystals appeared in 1−4 days and grew to 400−600 μm in length. All crystals were isomorphous with either the large or small unit cell forms of the *L. casei* TS apoenzyme (Finer-Moore et al., 1993).

Testing for Deamination of dCMP in Crystallization Drops. Any fortuitous deamination of dCMP would be undetectable by crystallographic means. Therefore, in order to test whether deamination of dCMP to dUMP occurred during crystallization, mother liquor from crystal drops containing wild-type TS with a high concentration of dCMP (20 mM) was separated isocratically on an Altex Ultrasphere IP column (4.6 mm × 25 cm) on a Hewlett-Packard 1090 HPLC equipped with a diode array detector. The eluant was 5 mM KH_2PO_4 and 5 mM tetra-*n*-butylammonium sulfate buffer, pH 7.0, with 5% acetonitrile. Absorbance spectra between 200 and 400 nm were collected for all peaks. For more rigorous testing, crystals from 10 sets of 10 μL drops of wild-type TS (60 μM) with dCMP (20 mM) were collected and redissolved in TS assay buffer (Liu & Santi, 1992). Fresh TS and cofactor were introduced to half of the redissolved solution to check for any dTMP formation. Both portions were then analyzed by HPLC. Under our HPLC conditions, retention times for dCyd, dUrd, dCMP, dUMP, and dTMP are 3.8, 4.5, 11.9, 15.8, and 20.8 min, respectively.

X-ray Data Collection. I_{hkl} data for most structures were collected on an R-axis IIC image plate detector system mounted on a Rigaku 18 kW generator run at 60 kV, 50 mA, collimated to 0.3 mm, using 1.0−2.0° wide frames in ω. The crystal to detector distances ranged from 22 to 24 cm. Data were reduced using R-axis II data reduction programs (Higashi, 1990; Sato et al., 1992).

I_{hkl} data for TS N229C bound to dUMP were collected on a Siemens IPC area detector coupled to a Siemens three-circle goniometer mounted on a Rigaku rotating target tube using monochromated Cu Kα radiation. A crystal to detector distance of 28 cm was used, and 2θ was set at 23°. Scan widths were 0.1° in ω. Data frames were processed by a modified version of the data collection software of Blum et al. (1987). Data were reduced to intensities using XDS (Kabsch, 1988).

Structure Solution Refinement. Structures were solved by difference Fourier methods starting with the structure of the *L. casei* apoenzyme (Finer-Moore et al., 1993). dUMP or dCMP was fitted to density in the first $(F_o - F_c)\alpha_{calc}$ maps. In addition, $(F_o - F_o)\alpha_{calc}$ maps were calculated between wild-type and mutant data sets. These maps are an especially sensitive method of determining shifts in structure. Water molecules were identified in subsequent difference density maps. Structures were refined by fitting to $(2F_o - F_c)\alpha_{calc}$ and $(F_o - F_c)\alpha_{calc}$ electron density maps using FRODO (Jones, 1985) or CHAIN (Sack, J. S., 1988) and then running molecular dynamics coupled with *R*-factor and energy minimization (X-PLOR) (Brunger et al., 1987). After partial refinement of the structures, $(F_o - F_c)\alpha_{calc}$ omit maps (calculated with the ligand omitted from phasing) were calculated, and dUMP or dCMP was refitted to the difference density. Data statistics and refinement statistics are compiled in Tables 1 and 2.

Comparison of Structures. Where direct difference electron density maps were computed [$(F_o - F_o)\alpha_{calc}$ maps], the relative positional shifts of atoms in two compared structures were accurately calibrated by comparison of integrated difference electron density with computed rms density in the noise regions of the map. This procedure gives accuracy in computed shifts of position that are ~10-fold more accurate than the positional uncertainty of atoms themselves.

The crystal structures we report here had slightly different cell constants from each other and from wild-type TS·dUMP. The *c*-axes for wild-type TS·dCMP, TS N229D·dUMP, and TS N229C·dUMP were 242 Å, compared to 230 Å for TS N229D·dCMP, 231 Å for TS N229C·dCMP, and 240 Å for wild-type TS·dUMP. For the purpose of comparison, coordinates of TS·dCMP and the TS N229D and TS N229C complexes were overlapped with wild-type TS·dUMP coordinates by a least-squares fit of the backbone atoms.

The significance of the differences between atoms in the overlapped structures was then evaluated as a function of the atomic *B*-factors (B) of the compared atoms using an equation of the form $\sigma(x,y,z)\ (B) = (aB^2 + bB + c)$, where

Table 2: Crystallographic Refinement Statistics

	WT·dUMP	WT·dCMP	N229D·dUMP	N229D·dCMP	N229C·dUMP	N229C·dCMP
parameters						
no. of atoms	2667	2659	2660	2699	2644	2672
no. of waters	54	46	47	86	33	64
diffraction agreement						
resolution (Å)	7−2.55	7−2.3	8−2.5	7−2.5	7−2.74	7−2.5
$I/\sigma(I)$ cutoff	2.0	1.0	1.0	1.0	1.0	1.0
no. of reflections	9566	13219	10441	11363	8609	11069
completeness (%)	67	67	69	77	72	76
completeness to 3 Å (%)	79	86	86	83	83	84
R_{crys} (%)	18.5	21.3	19.4	18.4	18.5	18.0
rms deviations from stereochemical ideality						
bond lengths (Å)	0.008	0.010	0.008	0.007	0.011	0.007
bond angles (deg)	1.7	1.6	1.6	1.6	2.0	1.6
torsion angles (deg)	24.7	24.8	24.6	24.7	25.7	24.8
av B (Å^2)	31.0	21.9	22.5	29.7	29.5	31.2
av B, dUMP or dCMP (Å^2)	26.2	43.0	44.4	37.2	46.2	25.0

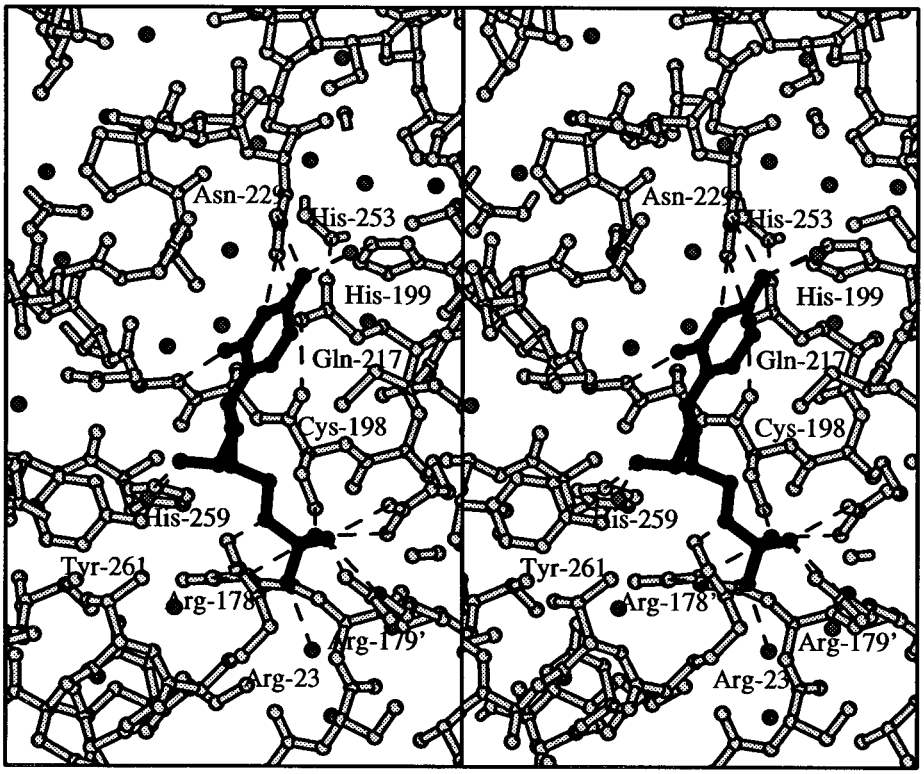

FIGURE 1: Stereo diagram of the dUMP binding site in *L. casei* TS. Selected residues in the active site are labeled. Hydrogen bonds between dUMP and the protein or ordered water are shown with dashed lines. Waters are shown as dark spheres. All stereo figures in this paper were made with MOLSCRIPT (Kraulis, 1991).

a, *b*, and *c* are empirically determined constants (Chambers & Stroud, 1979; Perry et al., 1990; Stroud & Fauman, 1995).

RESULTS

Geometry of the Pyrimidine Binding Site in Wild-Type TS·dUMP. In wild-type TS, dUMP binds on one side of the spacious active site cavity, close to the catalytic cysteine, Cys-198. The pterin ring of the cofactor, CH_2-H_4folate (or quinazoline ring of cofactor analog 10-propargyl-5,8-dideazafolate), binds directly on top of and parallel to the dUMP base; thus the kinetics of cofactor binding are, as expected, sensitive to dUMP orientation. Atom 4-O of the pyrimidine ring of dUMP fits in a pocket formed by one end of the central hydrophobic helix, which forms the core of the protein, and residues in the second and third β-strands of the very unusual, kinked β-sheet, which forms the dimer interface as well as the back wall of the active site cavity (Hardy et al., 1987). The pocket is lined by four highly conserved residues (Figure 1). Asn-229 and Cys-198 are invariant across species, while Gln-217 and His-199 are conserved in 25 out of 27 sequences. The orientation of the Asn-229 carboxamide group is fixed by a hydrogen bond from Oδ1 to Gln-217 Nϵ2. Gln-217 Nϵ2 also forms an ideal hydrogen bond to the carbonyl of Ser-219, a hydrogen bond acceptor; thus the orientation of the Gln-217 carboxamide group is unambiguous. It is unlikely that the Asn-229 and Gln-217 carboxamide groups would simultaneously flip 180° at the cost of the hydrogen bond to Ser-219 O, since the latter hydrogen bond helps maintain the unusual β-kink structure that matches a bend in the β-sheet at one wall of the active site cavity (Montfort et al., 1990). Gln-217 Oϵ2 is hydrogen bonded to His-253, although neither His-253 nor the hydrogen bond to Gln-217 Oϵ2 is conserved in other species.

Conserved His-199 is surrounded by several hydrogen-bonding groups, including conserved water molecules, and the His-199 Cβ−Cγ dihedral angle, which is determined by the imidazole ring orientation, is sensitive to location of ligands in the active site (unpublished observations). Since in TS·dUMP more than one hydrogen-bonding scheme from His-199 is possible, the identities of the His-199 imidazole nitrogen atoms have been assigned on the basis of analogy to *E. coli* TS ternary complexes, where His-199 Nδ1 is hydrogen bonded to Tyr-233 Oη and Nϵ2 is hydrogen bonded to an ordered water (Montfort et al., 1990). With this assignment of nitrogen atoms, His-199 Nδ1 hydrogen bonds to a water molecule (d = 3.0 Å).

C−H hydrogen bonds are often formed with histidine side chains, and His-199 utilizes a C−H hydrogen bond in the active site. His-199 Cϵ1 is 3.0 Å from dUMP 4-O; on the basis of observations of hydrogen bonds between carbonyl groups and Cϵ1 of histidines in other proteins (Derewenda et al., 1994), the interaction between dUMP 4-O and His-199 is also a C−H hydrogen bond.

TS Binds dCMP: Crystallography and Chromatography. Since dCMP binds poorly to wild-type TS ($K_d \sim 200$ μM), a high concentration of dCMP (~20 mM) was used for crystallization of the TS·dCMP complex. However, conversion of just 0.1% of dCMP to dUMP ($K_d \sim 0.4$ μM) (that is, replacement of 4-NH_2 by 4-O) would have resulted in a binary complex of wild-type TS with dUMP. To make certain that there was no dUMP in the crystals, crystals from a total of 100 μL of drops, containing 60 μM wild-type TS and 20 mM dCMP, were collected, washed, and redissolved in TS assay buffer. Part of the solution was analyzed on HPLC, and no dUMP could be detected. TS and cofactor were added to the rest of the solution, and HPLC analysis showed that no dTMP formed, which also suggests that no significant deamination occurs in this crystallographic structure.

As further proof that TS·dCMP cocrystals were not contaminated with dUMP, mother liquors were analyzed on HPLC. No dUMP was detected; however, we found nucleosides deoxycytidine (dCyd) and deoxyuridine (dUrd) in the mother liquor, and the amount increased with time. For a typical crystallization of wild-type TS with dCMP, about 2% of dCMP was converted to dUrd in 2 weeks. Therefore, we were careful to use only fresh crystals for X-ray data collection. These nucleosides do not bind well to TS. K_i for dUrd is >50 mM; thus we can be very confident that we are seeing TS·dCMP, with no competition from TS·dUrd in our crystal structure.

To be certain about species present in the mutant structures, nucleoside production was again assessed by HPLC. The same hydrolysis and deamination reactions that produced dCyd and dUrd in solution also occurred in drops of dCMP with TS N229D and TS N229C, as well as in a preparation of the TS mutant C198L. It has been reported that, in *E. coli* protein extracts, dCMP deaminase activity is not detectable while dCyd deaminase activity is very high (Wentworth & Wolfenden, 1978; Maley, 1978). The fact that only dUrd was detected in our samples, and not dUMP, fits these observations very well. Further purification of TS N229D protein by a Mono-Q column (Pharmacia) reduced both activities. We conclude that deamination of dCyd to dUrd does not result from TS itself, but from some contaminating enzymes.

"Nonproductive" Binding of dCMP by Wild-Type TS: Cytosine 4-NH_2 Is Forced Outside of the Pyrimidine Binding Pocket. A difference electron density map, computed with terms $(F_o - F_c)\alpha_{calc}$, where the phases α_{calc} are derived from unliganded *L. casei* TS, clearly shows that dCMP bound in the active site. While the density for dCMP is weaker than that seen for dUMP in omit maps for dUMP binary complexes, the dCMP is not disordered and the substituents on the pyrimidine and ribose rings are well-defined (Figure 2). The pyrimidine ring is tilted away from the binding site for the dUMP base such that it impinges on the cofactor binding site (Figure 3). Atom 4-NH_2 is outside the pocket formed by Cys-198, His-199, Gln-217, and Asn-229, wedged between the Asn-229 side chain and backbone atoms on the core hydrophobic helix. Gly-225 Cα is about van der Waals distance (3.6 Å) from 3-N of dCMP. The repositioning of the pyrimidine ring relative to the dUMP base is a significant but not drastic change. 4-NH_2 of dCMP is 2.2 Å from where 4-O binds in dUMP (Figure 2), which is approximately four times the uncertainty in the differences between two equivalent atoms of the TS·dUMP and TS·dCMP crystal structures, taking *B*-factors and resolution of the structures into account (Perry et al., 1990; Stroud & Fauman, 1995). Deoxycytidine base atoms 4-C, 5-C, and 6-C are all shifted by a distance of at least 3 standard deviations from the positions of the equivalent atoms in dUMP. The dCMP pyrimidine is in the *anti* conformation, as is dUMP bound to TS. The orientation around the C4′−C5′ bond is *trans*, *gauche*, as in bound dUMP, but the dihedral angle around C5′−O5′ is 91° compared to 170° in the dUMP binary complex.

Two out of three hydrogen bonds to the pyrimidine ring are absent in the dCMP binary complex: Asn-229 Oδ1−dUMP 3-NH and Asn-229 Nδ2−dUMP 4-O. Only the hydrogen bond between 2-O and Asp-221 NH is present. 3-N is 3.3 Å from Oδ1 of TS N229 and cannot hydrogen bond to TS N229. The amino substituent of dCMP, 4-NH_2, is 3.15 Å from the Nδ_2 atom of Asn-229 and 4.8 Å from His-199. Since Asn-229 Nδ2 and dCMP 4-NH_2 are both proton donors, we assume they do not form a hydrogen bond. However, when positions for the hydrogen atoms on these groups are estimated from the geometry of the heavy atoms, they are close to van der Waals distance from the neighboring heavy atom. 4-NH_2 is hydrogen bonded to an ordered water; however, it is not the conserved water bound to 4-O of dUMP in TS·dUMP complexes. 6-C in the pyrimidine base is 4.4 Å from the catalytic sulfhydryl, Cys-198 Sγ. Cys-198 Sγ is positioned over 6-C of the pyrimidine ring with the angle Sγ−C6−C5 = 107°, compared to Sγ−C6−C5 = 90° in TS·dUMP. Thus, the catalytic sulfhydryl is favorably oriented for attack at 6-C of dCMP but is about 1 Å further from 6-C in the dCMP complex than in the dUMP complex. In the dUMP complex, 4-O of dUMP makes a 2.9 Å hydrogen bond to Asn-229 Nδ2 and is 3.0 Å from His-199. 3-NH of dUMP hydrogen bonds to Asn-229 Oδ2, and 6-C is 3.3 Å from Cys-198 Sγ.

The two conserved hydrogen bonds to the ribose hydroxyl group, OR3′, seen in TS complexes with dUMP, one from Tyr-261 and the other from His-259, are present in the TS·dCMP complex. As in TS·dUMP, the phosphate group of dCMP is extensively hydrogen bonded to surrounding arginines 23, 178′,[2] 179′, and 218 and a conserved water.

Asn-229 has adjusted its conformation to accommodate the dCMP. The Cβ−Cγ dihedral angle of the Asn-229 side

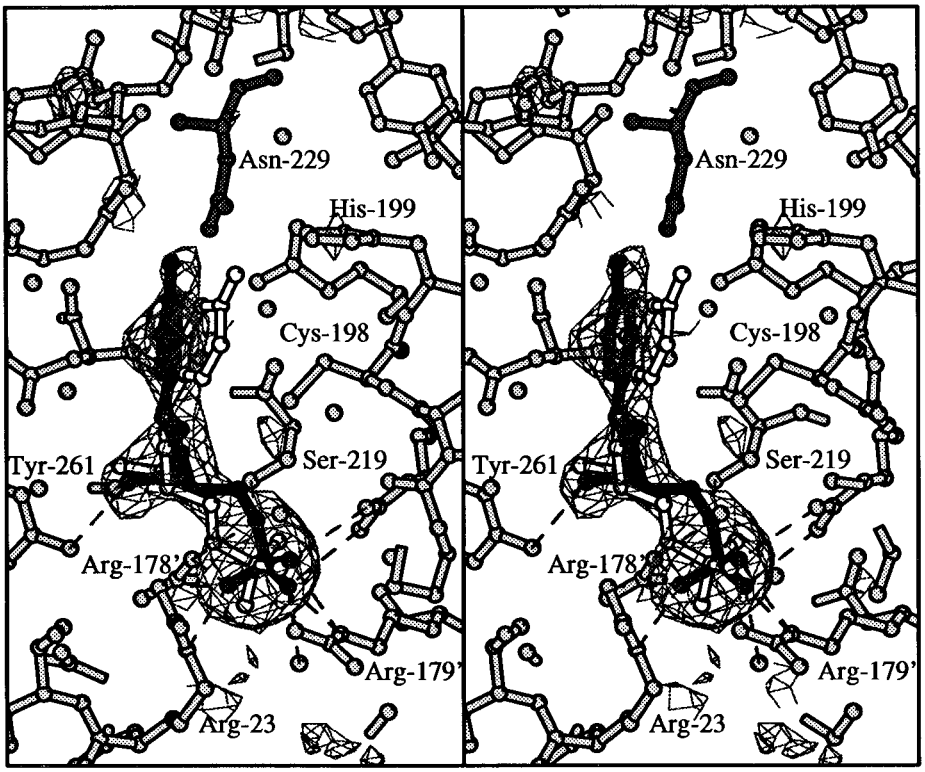

FIGURE 2: Stereo diagram of an omit map showing electron density for dCMP bound to the active site of *L. casei* TS. The omit map is contoured at 2.5σ. The position of dCMP has been refined to the center of the cage of density surrounding it, and the error in the position of an atom in the pyrimidine ring is on the order of $\pm$0.2 Å. dUMP from wild-type TS (white bonds) is overlaid on the diagram for comparison. In this and subsequent figures, overlap of ligands was accomplished by least-squares fit of the atoms in one protein structure to those in the other. Hydrogen bonds between dCMP and the protein or ordered water are drawn with dashed lines.

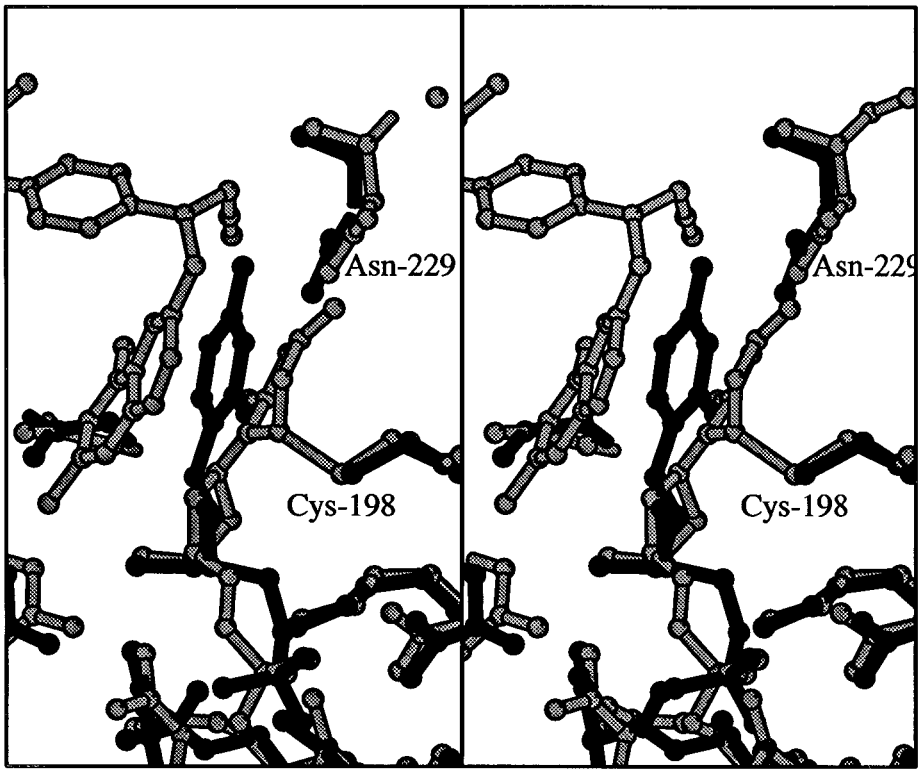

FIGURE 3: Same structure as in Figure 2 (in black bonds) superimposed on the *E. coli* TS ternary complex with dUMP and a cofactor analog (Montfort et al., 1990) (in gray bonds).

chain changes by 16° with respect to Asn-229 in TS·dUMP, rotating the asparagine carboxamide group to make room for the dCMP amino group. The resulting changes in the positions of Oδ1 and Nδ2 are significant at the 2σ level (Perry et al., 1990; Stroud & Fauman, 1995). Hydrogen bonds between Gln-217 Nϵ2, Asn-229 Oδ1, and Ser-219 O are maintained; this indicates that the Asn-229 carboxamide has not reversed its orientation to allow it to hydrogen bond

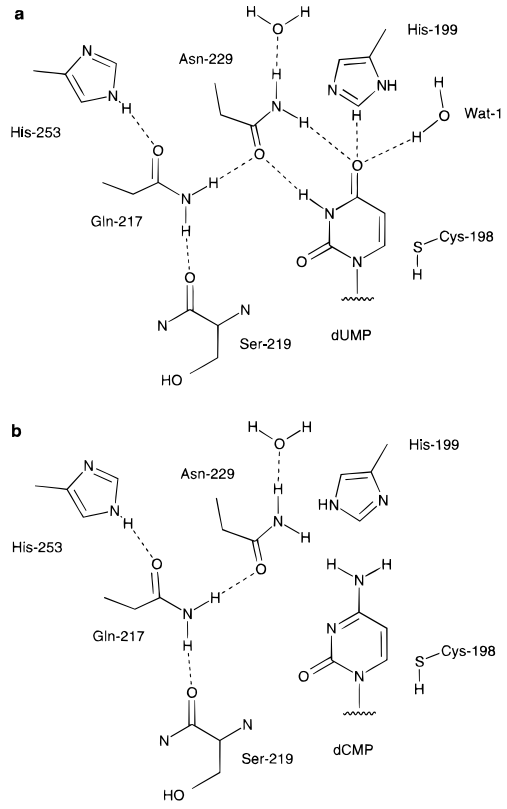

FIGURE 4: (a) Diagram of a hydrogen bond network between Asn-229, Gln-217, Ser-219, His-253, and 3-NH and 4-O of dUMP. (b) When the hydrogen bond network in the protein is maintained, Asn-229 cannot hydrogen bond to dCMP 3-N or 4-NH_2.

to the dCMP pyrimidine (Figure 4). His-199 Nϵ2 is 2.8 Å from Asn-229 Nδ2, and if protonated, its hydrogen is pointed perpendicular to the Asn-229 carboxamide plane and is hydrogen bonded to the Nδ2 lone electron pair.

TS N229C: Removing Constraints on Pyrimidine Binding Favors the "Productive" Orientation of Nucleotide in Complexes with dUMP and dCMP. When Asn-229 is mutated to a cysteine, the side chain of Cys-229 is rotated around the Cα−Cβ bond such that the Sγ atom is in a small space between the hydrophobic helix and the β-sheet (Figure 5). This small pocket is directly above the pyrimidine base binding pocket and is lined with mainly hydrophobic residues, Tyr-233, Phe-251, Leu-215, Gln-217, and His-253.

There are no significant differences between the positions of the atoms in the dUMP pyrimidine ring compared to the dUMP base in the wild-type TS·dUMP crystal structure. dUMP 4-O is hydrogen bonded to an ordered water. The distance between 6-C and the active site sulfhydryl is 3.5 Å, compared to 3.3 Å in the wild-type complex, and the Sγ−C6−C5 angle is 94°, close to the value in the wild-type TS complex. dUMP 2-O is hydrogen bonded to Asp-221 N, as in other dUMP complexes. The conserved hydrogen bonds between the ribose 3′-O atom and residues Tyr-261 and His-259 are also present. The phosphate moiety of dUMP is in the usual phosphate binding site. Arg-23, which is a well-ordered dUMP-binding residue only in ternary complexes of TS (Finer-Moore et al., 1996), is oriented further from the phosphate moiety and makes only one hydrogen bond to the phosphate oxygen atoms. The structure of TS N229C·dUMP is very close to the structure of TS N229V·dUMP predicted by molecular mechanics calculations (Rastelli et al., 1995), supporting that enthalpic forces drive the association.

The binding site for dCMP in N229C is slightly different from the dUMP binding sites in either TS N229C or in wild-type TS. In the TS N229C·dCMP structure, the pyrimidine ring lies close to the pyrimidine binding site but is translated ~1.0 Å downward from His-199 (as viewed in Figure 1), presumably as a result of steric interactions between the His-199 imidazole ring and dCMP 4-NH_2 (Figure 5). Thus every atom in the dCMP base is shifted relative to the corresponding dUMP atom in the TS·dUMP crystal structure, and these differences are about 2.5 times their expected error, based on the *B*-factors and resolution of the crystal structures (Perry et al., 1990; Stroud & Fauman, 1995). 6-C is ~3.5 Å from Cys-198 Sγ and Sγ−C6−C5 = 95°, but 4-NH_2 of dCMP is 3.3 Å from the closest atom in the His-199 side chain (compared to 3.0 Å for dUMP bound to wild-type TS or TS N229C). No hydrogen bonds to dCMP 4-NH_2 are apparent in the crystal structure. There are no ordered waters within 3.4 Å of dCMP 4-NH_2; however, there is an ordered water hydrogen bonded to dCMP 3-N. The conserved hydrogen bonds to the ribose ring, phosphate group, and 2-O of the base are present. Thus removing the Asn-229 side chain eliminates hydrogen bonds to the pyrimidine ring that maintain a precise orientation of the nucleotides in the active site.

TS N229D Complexes: "Productive Site" Binding for both dCMP and dUMP, with Hydrogen Bonds to Asp-229. When Asn-229 is mutated to an aspartic acid, which is isosteric with the asparagine, the His-199 imidazole ring rotates ~45° toward the Asp-229 carboxyl group and is probably hydrogen bonded to it. The change in orientation of the His-199 imidazole is significant at the 3σ level (Perry et al., 1990; Stroud & Fauman, 1995). His-199 Nϵ2 is 2.9 Å from Asp-229 Oδ2, and if protonated, the Nϵ2 hydrogen is oriented perpendicular to the plane of the Asp-229 carboxyl. His-199 Nδ1 is hydrogen bonded to Tyr-146 Oη. Asp-229 Oδ1 forms the conserved hydrogen bond to Gln-217 Nϵ2, analogous to the hydrogen bond between Asn-229 and Gln-217 in wild-type TS.

In the structures of TS N229D·dUMP and TS N229D·dCMP, dCMP and dUMP are in similar positions to that of dUMP in wild-type TS, but with the pyrimidine base tilted away from His-199 such that the 4-C substituent in both ligands (4-O in dUMP and 4-NH_2 in dCMP) is ~4 Å from the His-199 imidazole ring, compared to 3 Å in wild-type TS·dUMP (Figures 6 and 7). The ~1 Å displacement of the 4-C substituents is small but significant at the 3σ level (Perry et al., 1990; Stroud & Fauman, 1995). An $(F_o1 - F_o2)\alpha_{calc}$ difference map, computed with coefficients $|F_o1|$, the amplitudes from wild-type TS·dUMP, minus $|F_o2|$, the amplitudes from TS N229D·dCMP, reveals the differences between TS·dUMP and TS N229D·dCMP crystal structures more sensitively than the comparison of their refined coordinates (Figure 8). This difference map clearly shows the shift in the position of the 4-NH_2 atom in TS N229D·dCMP relative to 4-O in TS·dUMP and also indicates that, in TS N229D·dCMP, Cys-198 may be statistically disordered, with two rotomers represented in the crystal structure.

[2] A prime following a residue number signifies that the residue belongs to the second protomer in the TS dimer, i.e., the protomer that is not currently being discussed.

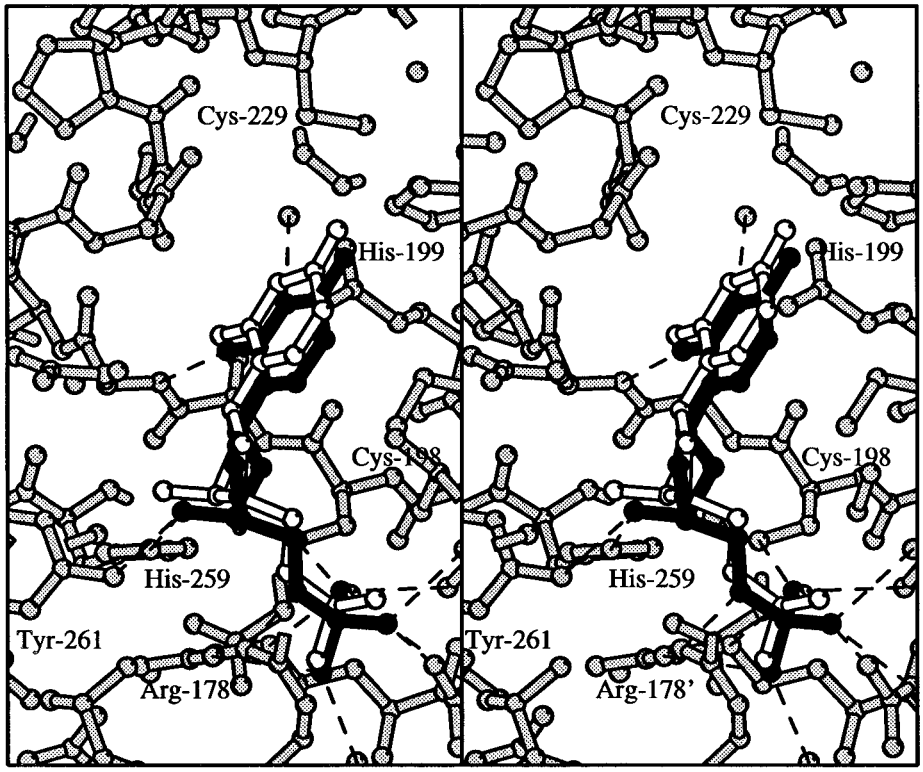

FIGURE 5: Stereo diagram of dCMP (black bonds) bound to the active site of *L. casei* TS N229C. dUMP from wild-type TS (white bonds) is overlaid. Hydrogen bonds between dUMP and the protein or ordered water are shown with dashed lines.

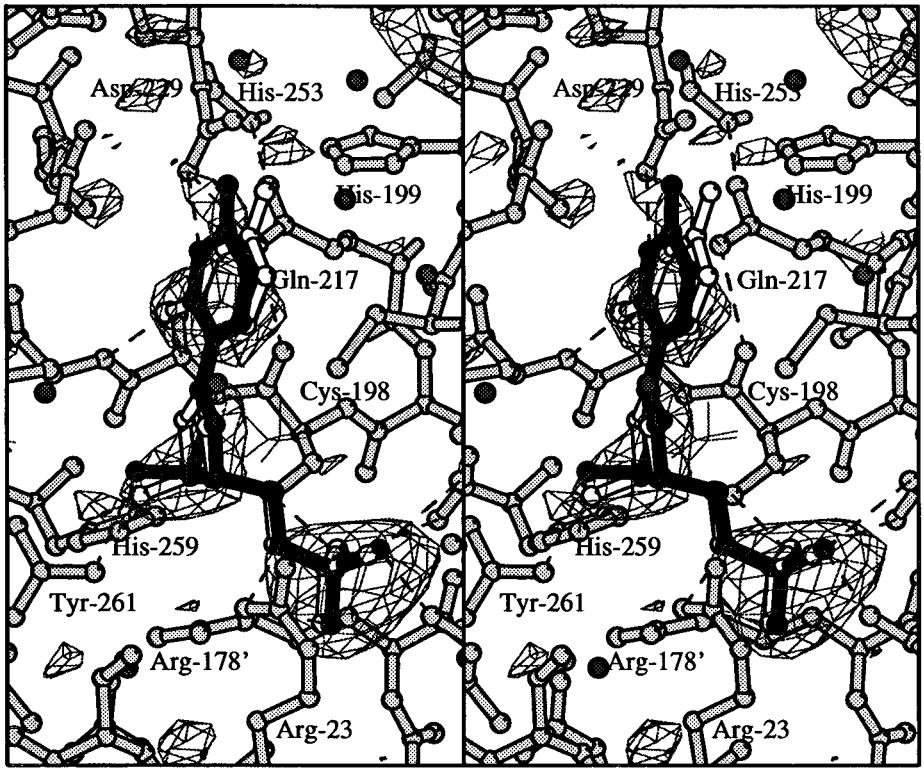

FIGURE 6: Stereo diagram of an omit map showing difference electron density for dUMP bound to TS N229D. The density map is contoured at 2.5σ. dUMP from wild-type TS (white bonds) is superimposed on the active site. Hydrogen bonds between dUMP and the protein or ordered water are shown with dashed lines.

In the crystal structure of TS N229D·dCMP, the imidazole of His-199 is in van der Waals contact with the 4-amino substituent on the pyrimidine ring (Figure 9), and 6-C of dCMP is 3.9 Å from the active site sulfhydryl, Cys-198 Sγ. In TS N229D·dUMP, on the other hand, the less bulky 4-carbonyl group is not in van der Waals contact with His-199 (Figure 10). The C6−Cys-198 Sγ distance is 3.4 Å, close to the distance in the wild-type complex. The Sγ−C6−C5 angle is 120° and 113° for TS N229D·dUMP and TS N229D·dCMP, respectively. Both ligands are in an essentially identical conformation to bound dUMP in the wild-type complex. Each makes the conserved hydrogen

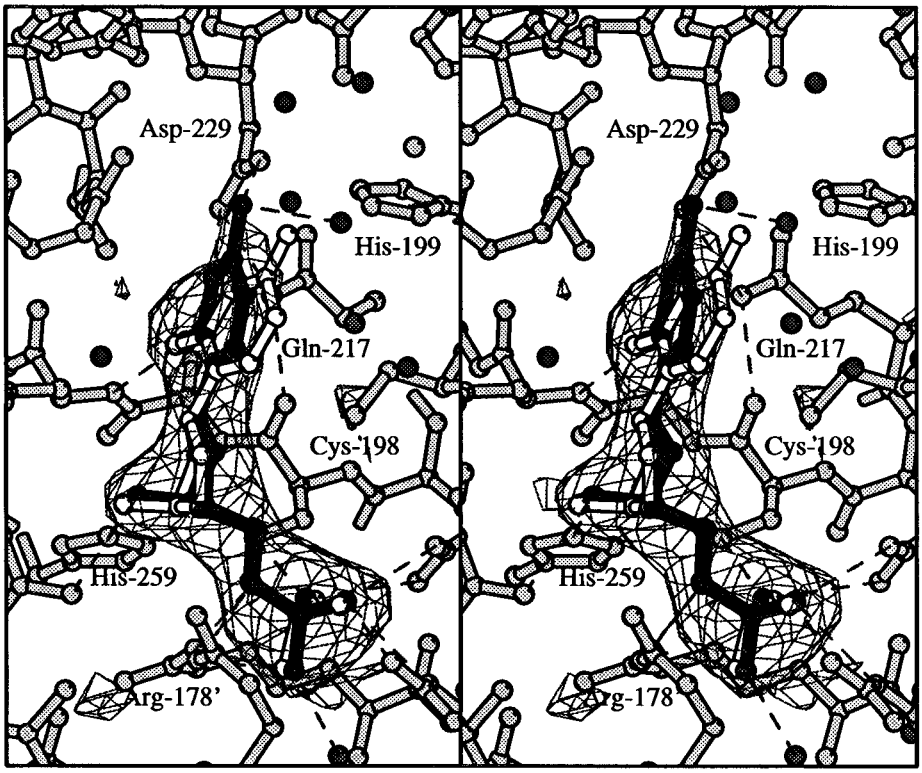

FIGURE 7: Stereo diagram of an omit map showing difference electron density for dCMP bound to TS N229D. The density map is contoured at 2.5σ. dUMP from wild-type TS (white bonds) is superimposed on the active site. Hydrogen bonds between dUMP and the protein or ordered water are shown with dashed lines.

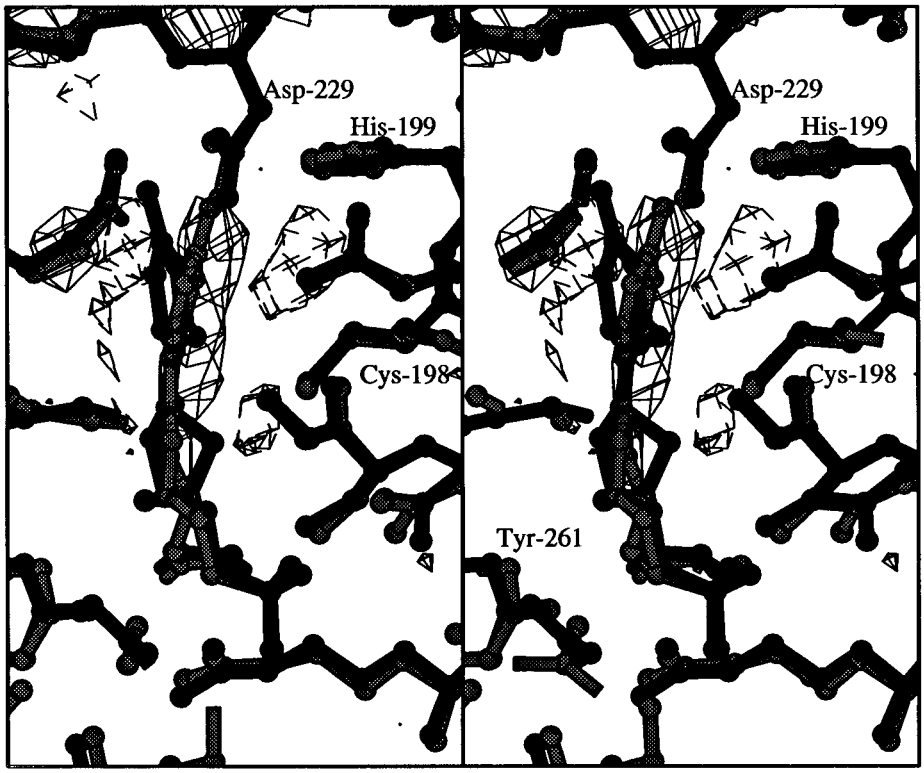

FIGURE 8: Difference density map calculated with coefficients ($|F_o1| - |F_o2|$), where $|F_o1|$ is a structure factor amplitude for TS·dUMP crystallized in the small unit cell form (Finer-Moore et al., 1993), which is isomorphous to the TS N229D·dCMP crystals, and $|F_o2|$ is the corresponding structure factor amplitude from the TS N229D·dCMP crystal structure. Phases were calculated from the TS·dUMP structure. Negative density is shown with broken lines and positive density with unbroken lines. The TS·dUMP crystal structure is plotted with gray bonds, and the TS N229D·dCMP crystal structure is plotted with black bonds. The map sensitively indicates differences between the two structures that cannot always be reliably detected by comparison of refined coordinates. For example, a negative density peak above the Cys-198 side chain may indicate a second rotamer for Cys-198 in TS N229D·dCMP crystals.

bonds between protein and 2-O of the base, 3′-O of the ribose ring, and the oxygen atoms of the phosphate moiety. 4-NH_2 of dCMP is hydrogen bonded to the conserved, ordered water that is also present in wild-type TS binary and ternary

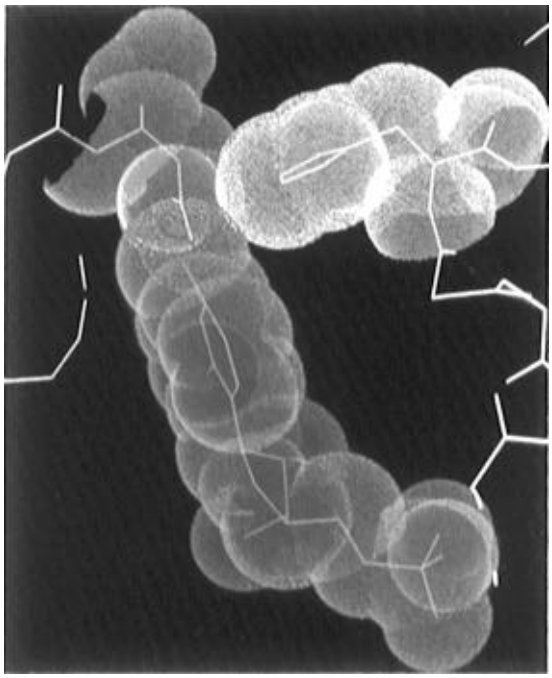

FIGURE 9: Midas Plus drawing (Ferrin et al., 1988) of the active site of TS N229D·dCMP with van der Waals surfaces drawn around dCMP, Asp-229, and His-199.

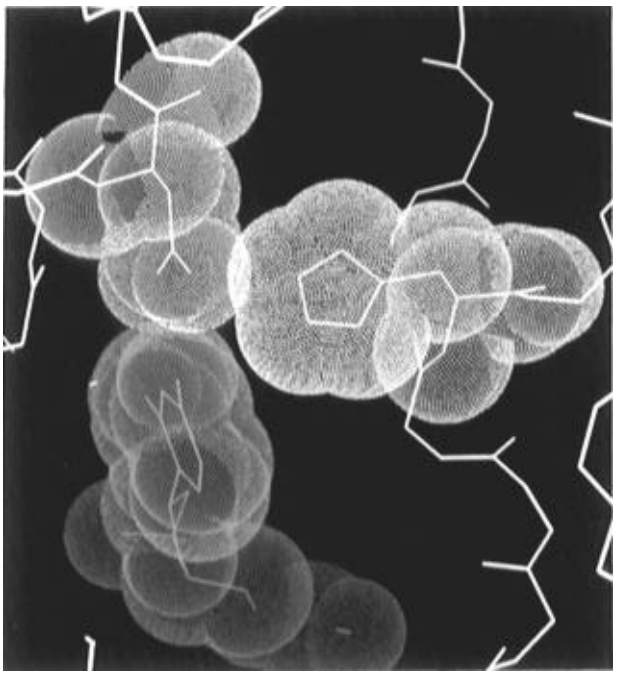

FIGURE 10: Midas Plus drawing (Ferrin et al., 1988) of the active site of TS N229D·dUMP with van der Waals surfaces drawn around dUMP, Asp-229, and His-199. The 4-O of dUMP has a smaller van der Waals radius than the 4-NH_2 moiety of dCMP and therefore is not in contact with His-199.

complexes. There are several ordered waters in the vicinity of the residues surrounding 4-O of dUMP, but none are in hydrogen-bonding distance to 4-O.

Hydrogen bonding between Asp-229 and the pyrimidine ring of dUMP or dCMP is ambiguous because it is impossible to tell from the crystallographic data whether this residue is protonated. The pH of the crystal is ~7 and aspartic acid normally has a pK_a of ~4, but the pK_a of an aspartate can be affected by its environment in the protein (Davies, 1990; Langsetmo et al., 1991). In its unprotonated state, Asp-229 is capable of making only one hydrogen bond to either dCMP or dUMP. Distances between 3-N and 4-NH_2 of dCMP and the carboxyl oxygen atoms of Asp-229 are 2.9 and 2.7 Å, respectively. Thus the expected hydrogen bond to the amino substituent is present, and a hydrogen bond to 3-NH possibly exists.

Distances between 3-NH and 4-O of dUMP and the Asp-229 carboxyl oxygen atoms are similar. Given the expected accuracy of the distances between atoms calculated from this 2.5 Å structure, the contact to 4-O could be either a van der Waals contact (~2.8 Å) or a hydrogen bond, depending on the protonation state of Asp-229. A hydrogen bond from Asp-229 to 3-NH is expected and, based on geometry of the heavy atoms, exists.

Molecular dynamics calculations predict the dUMP and dCMP binding sites in TS N229D to be highly dependent on the protonation states of His-199 and Asp-229 (Rastelli et al., 1995). Comparison of the crystal structures of TS N229D·dUMP and TS N229D·dCMP with the molecular mechanics results gives some insight into the protonation states of these two residues. The crystal structure of TS N229D·dCMP closely resembles the molecular mechanics structure calculated assuming a neutral Asp-229 and the δH tautomer (atom Nδ1 protonated) of His-199, except that there is no ordered water hydrogen bonded to 4-NH_2 in our structure. In the structures predicted by molecular mechanics for TS N229D·dCMP with a negatively charged Asp-229, dCMP and/or Asp-229 have shifted such that 3-N is not at hydrogen-bonding distance from Asp-229 Oδ. Our structure is therefore more consistent with a neutral Asp-229. Indeed, a proposal for the mechanism of methylation of dCMP by TS N229D requires that Asp-229 be protonated (Liu & Santi, 1992).

The molecular mechanics results are less helpful in distinguishing between neutral or charged Asp-229 in the TS N229D·dUMP complex. The TS N229D·dUMP crystal structure resembles both the molecular mechanics structure calculated with neutral Asp-229 and the δH tautomer of His-199 and the structure calculated with a charged Asp-229 and the ϵH tautomer of His-199; no simulation was done with a neutral Asp-229 and the ϵH tautomer of His-199.

Table 3: Kinetic and Binding Data for Wild-Type TS, TS N229C, and TS N229D[a]

	(a) TS Activity				
	k_{cat} (s^{-1})	K_m(dUMP) (μM)	K_m(CH_2-H_4folate) (μM)	k_{cat}/K_m(dUMP) (s^{-1} μM^{-1})	K_d(dUMP) (μM)
WT	3.6	5.0	10.0	0.72	0.38
TS N229C	0.22	17.0	92.0	0.013	1.6
TS N229D	0.004	50.0	35.0	0.00007	2.7
	(b) dCMP Methylase Activity				
	k_{cat} (s^{-1})	K_m(dCMP) (μM)	K_m(CH_2-H_4folate) (μM)	k_{cat}/K_m(dCMP) (s^{-1} μM^{-1})	K_d(dCMP) (μM)
WT	nd[b]				160
TS N229C	nd[b]				0.49
TS N229D	0.45	150	170	0.003	2.8

[a] Assays and data reported in Liu and Santi (1992, 1993a,b). [b] No detectable activity.

DISCUSSION

The Asn-229 Side Chain Discriminates against dCMP Binding. Table 3 lists kinetic parameters, which focus on catalytic effectiveness, and binding data gained from competition for a noncatalytic inhibitor, which therefore focus

on binary complex interaction energies, for the wild-type enzyme and the two N229 variants whose structures we report here. Mutations of Asn-229 to hydrophobic residues Trp, Leu, Ile, Val, Met, and Cys affect k_{cat} less than 10-fold for dUMP, while other substituents, including Asp, reduce k_{cat} over 10^3-fold, with a relatively small change (<10-fold) in K_m (Liu & Santi, 1993b). The only mutants with any measurable k_{cat} for dCMP are N229D and N229E (Liu & Santi, 1993a). However, N229 mutation affects the ratios of K_d for dUMP to dCMP from 1:400 for Asn-229 (wild-type enzyme) to close to 1:1 for most mutants (Liu & Santi, 1993a). Thus the presence of Asp at Asn-229 inhibits catalysis for dUMP, and the absence of Asn-229 favors binding of dCMP almost to wild-type dUMP levels.

The K_d for dCMP in the wild-type enzyme, 160 μM, is almost the same as the K_d for 2-deoxyribose 5′-phosphate alone (unpublished). Thus any entropic gain from binding a larger substrate is balanced by a decrease in enthalpy on going from a fully solvated dCMP to enzyme-bound dCMP with no hydrogen bonds to 3-N and only one hydrogen bond (from ordered water) to 4-NH_2. The K_d for dCMP is also ~400-fold higher than the K_d for dUMP, suggesting that the enthalpic component of the improvement in binding dUMP over dCMP is worth $\Delta G_f^\circ \sim 3.6$ kcal/M (assuming similar entropic components in the binding energies). This energy difference is at least partially attributable to the two additional hydrogen bonds between Asn-229 and the base in the dUMP complex. In the two variants the K_d's for dCMP and dUMP are approximately equal and less than 10-fold higher than the K_d for dUMP in the wild-type enzyme. The crystal structures of the complexes reported here provide insight into the differences in K_d for dCMP in wild-type TS and in the TS variants.

In the wild-type dCMP complex, unfavorable interactions between the 3-N and 4-NH_2 nitrogen atoms of the dCMP base and the Asn-229 carboxamide group prevent dCMP from binding in an identical orientation to dUMP in wild-type TS. A network of hydrogen bonds between Gln-217, His-253, and the carbonyl of Ser-219 is evidently strong enough to prevent the carboxamide group of Asn-229 from rotating 180° to an orientation that could hydrogen bond to 4-NH_2 and 3-N of the dCMP base (Figure 4). However, the shift of dCMP relative to the dUMP binding site is not nearly as drastic as predicted by molecular mechanics calculations (Rastelli et al., 1995). Hydrogen bonds to 2-O of the pyrimidine ring and 3′-O of the ribose ring and many of the hydrogen bonds to the phosphate moiety of dCMP are preserved. The 4-NH_2 of the pyrimidine ring of dCMP is within van der Waals distance of the asparagine carboxamide group, and 3-N of dCMP is buried and about van der Waals distance from backbone atoms in the protein. The dCMP base and the Asn-229 side chain of TS are neither hydrogen bonded to each other nor fully exposed to solvent. Only 4-NH_2 of dCMP in the wild-type TS·dCMP complex is hydrogen bonded to ordered water. Thus going from the fully solvated unbound state to the bound state costs hydrogen-bonding energy. Possibly some distortion of dCMP geometry and unfavorable interactions of dCMP with surrounding residues also contribute to the increase in K_d for dCMP binding compared to dUMP binding.

When the side chain for Asn-229 is effectively removed from the active site cavity by mutation to a cysteine, the enzyme no longer selectively binds dUMP. The K_d for dCMP in TS N229C is approximately equal to the K_d for dUMP in the wild-type enzyme, and the K_d for dUMP is ~4-fold higher in this variant than in wild-type TS (Liu & Santi, 1993a) (Table 3). In the TS N229C complexes with dUMP and with dCMP there are no apparent unfavorable contacts with the pyrimidine bases. Further, even though the dUMP 3-NH and 4-O (or the dCMP 3-N and 4-NH_2) cannot hydrogen bond to protein side chains, they are fully exposed to solvent. The 4-O atom of dUMP in TS N229C·dUMP and the 3-N of dCMP in TS N229C·dCMP are each hydrogen bonded to ordered water. Compensation for the hydrogen bonds between dUMP and Asn-229 by solvent in TS N229C·dUMP is consistent with the small increase in K_d for dUMP for this variant over that for wild-type TS.

TS N229D binds both dUMP and dCMP with K_d values of ~3 μM (Liu & Santi, 1993a). The reason this variant no longer distinguishes between binding of the two substrates is that the hydrogen-bonding characteristics of aspartate are less restrictive than those of asparagine: either carboxyl oxygen of aspartate can accept a hydrogen bond. dCMP hydroxymethylase, an enzyme closely homologous to TS, which hydrogen bonds to the dCMP base via an aspartate at the 229 position, is less selective than TS. dCMP hydroxymethylase methylates both dCMP and dUMP, although the activity for methylation of dUMP is low (Graves et al., 1992). In another example of a carboxyl group being less selective in hydrogen bonding than a carboxamide, the (cytosine-5) DNA methyltransferase M. *Hha*I, which hydrogen bonds to 3-N and 4-NH_2 of cytosine via a glutamic acid residue (Klimasauskas et al., 1994), is able to methylate uracil if the substrate contains a G·U mismatch (Klimasauskas & Roberts, 1995). TS N229D makes at least one hydrogen bond between Asp-229 and the pyrimidine bases of dUMP and dCMP in the binary complex structures.

Wild-Type TS·dCMP: Can Small Distortions in Substrate Orientation Prevent Catalysis? In binary and ternary complexes of TS, the pyrimidine ring of dUMP is in a highly constrained orientation, hydrogen bonded to Asn-229 and close to or, in the case of *L. casei* TS·dUMP, hydrogen bonded to His-199. This orientation of the pyrimidine ring is optimal for formation of a covalent bond between 6-C of dUMP and Cys-198 Sγ and permits the cofactor to bind with its pterin ring parallel to and stacked on top of the pyrimidine ring, with its 5-N methylene group aligned with 5-C of dUMP (Montfort et al., 1990; Matthews et al., 1990). In TS·dCMP, dCMP is forced by steric effects out of this optimal orientation, and even though the deviation is only about 2 Å, it may compromise the ability of the enzyme to form a covalent ternary complex with enzyme and cofactor, as shown in Figure 3. In this case, energetic barriers to ternary complex formation alone may ensure that dCMP will not be a substrate for TS. Whether or not TS is able to form a covalent ternary complex with dCMP can be better ascertained by cocrystallization experiments with TS, dCMP, and a cofactor analog. Cocrystallization of *L. casei* TS with substrate and cofactor analogs is generally not successful, but the experiment can be done with *E. coli* TS.

Correlation between Catalysis and Hydrogen Bonding to 4-O (or 4-NH_2). The structure of TS N229C·dCMP shows dCMP bound in a very similar manner to dUMP in wild-type TS. 6-C is 3.4 Å from Cys-198 Sγ and well positioned for forming a covalent bond to this atom, as required in the

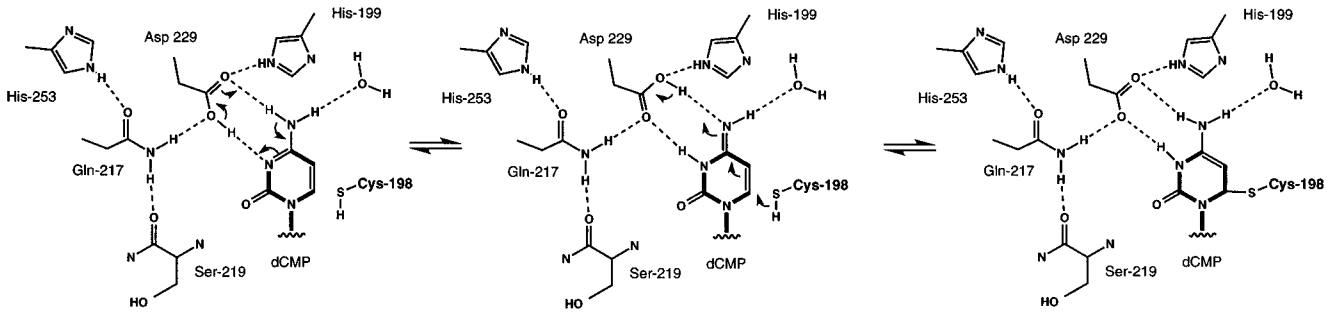

FIGURE 11: Diagram of hydrogen bonds around the dCMP base in TS N229D·dCMP, showing how the hydrogen bonds between dCMP and Asp-229 stabilize the imino tautomer of dCMP, thereby activating dCMP for covalent addition to Cys-198.

enzyme-catalyzed reaction. The cofactor binding site is open, and the pterin ring bound in its usual site would stack against the dCMP pyrimidine ring. Thus, there are no steric barriers to formation of a productive, covalent, complex of this variant with dCMP and cofactor, yet TS N229C does not catalyze methylation of dCMP. This result suggests that electronic factors, as well as optimal orientation of substrates, are required for dCMP methylase activity. Therefore, we propose (below) that hydrogen bonds to the dCMP base are required for catalysis.

The dCMP methylase activity of TS N229D, which is absent in all other variants we have assayed except for TS N229E (Liu & Santi, 1993a), probably results from hydrogen bonding between Asp-229 and the 3-N and 4-NH_2 atoms on the dCMP base. Hydrogen bonding between a neutral Asp-229 and 3-N and 4-NH_2 on dCMP stabilizes the reactive imino tautomer of dCMP, which is analogous to the keto tautomer of dUMP (Liu & Santi, 1992) (Figure 11). The geometry of interactions between dCMP and Asp-229 in our crystal structure is ideal for formation of these hydrogen bonds. We infer that the pK_a of Asp-229 is raised by its environment in the dCMP complex such that Asp-229 is protonated a greater proportion of the time, thus shifting the tautomeric equilibrium of dCMP and increasing the reactivity of dCMP toward methylation. Similarly, a substrate binding glutamic acid in DNA, (cytosine-5) methyltransferase *Hae*III, appears to hydrogen bond to 3-N and 4-NH_2 of cytosine in the crystal structure of this complex, determined at neutral pH, implying that its pK_a is also raised (Reinisch et al., 1995).

Hydrogen bonding between the Asp-229 carboxyl and dCMP brings 6-C closer to Cys-198, allowing for activation of dCMP by the active site cysteine. However, dCMP cannot form a hydrogen bond between its 4-amino substituent and Cϵ1H of His-199 analogous to the hydrogen bond between 4-O of dUMP and His-199 Cϵ1H in wild-type TS (Figures 1 and 4). His-199 instead sterically interferes with optimal orientation of dCMP for activation by Cys-198 (Figure 9). In the crystal structure of TS N229D·dCMP, the pyrimidine ring is still slightly outside the pyrimidine binding site, and 6-C is 4 Å from Cys-198 Sγ. Unfavorable interactions between dCMP and His-199 may partly account for the fairly high K_m of 150 μM for dCMP methylation by TS N229D.

Reversal of substrate specificity in the TS N229D variant is the result both of acquisition of dCMP methylase activity and of a 10^4-fold decrease in k_{cat}/K_m for dUMP methylation. In the TS N229D·dUMP structure, the pyrimidine base of dUMP is moved away from His-199 relative to its position in wild-type TS, as is dCMP in TS N229D. In this case, however, perturbation in dUMP orientation is probably not a result of steric interactions with His-199 since dUMP 4-O is not in van der waals contact with His-199 in the crystal structure of TS N229D·dUMP (Figure 10). A carbonyl oxygen is less bulky than an amino group, and 4-O of dUMP should be capable of hydrogen bonding to His-199 in TS N229D, as it does in wild-type TS. Therefore, we conclude that, in TS N229D·dUMP, the Asp-229 carboxyl, not the His-199 imidazole, prevents optimal orientation of dUMP. Thus, in TS N229D·dUMP, our evidence suggests that Asp-229 hydrogen bonds only to 3-NH of the dUMP base. Assuming hydrogen bonds to 4-O of dUMP are an important means of stabilizing intermediates during dUMP methylation, lack of hydrogen bonds to dUMP 4-O from either Asp-229 or ordered water may explain the 10^4 lower k_{cat}/K_m in TS N229D compared to wild-type TS. In contrast, 4-O of dUMP in the TS N229C·dUMP complex is hydrogen bonded to an ordered water, and this correlates with only a 56-fold lower k_{cat}/K_m for TS N229C (Liu & Santi, 1993b). Ultimately, it will be important to determine structures not only of binary complexes of the N229 mutants but also of ternary complexes with cofactor analogs and substrate in order to better evaluate the role of Asn-229 in catalysis.

CONCLUSION

The crystal structure of wild-type *L. casei* TS bound to dCMP demonstrates how steric and electronic properties of Asn-229 disfavor binding of dCMP. When the barrier presented by the Asn-229 side chain is eliminated by mutation to a smaller residue (cysteine) or a residue with less restrictive hydrogen-bonding properties (aspartic acid), both dCMP and dUMP bind close to the dUMP binding site in wild-type TS. The dUMP or dCMP methylation activities of the Cys and Asp variants correlate with the presence of hydrogen bonds to the 4-substituents of these two possible substrates. When no hydrogen bonds from side chain atoms or ordered water are made to the 4-O (or 4-NH_2) of dUMP (or dCMP), the variant has very low k_{cat}/K_m for methylation of that substrate.

ACKNOWLEDGMENT

Figures 9 and 10 were made using Midas Plus written by Conrad Huang, Eric Pettersen, and Greg Couch at the UCSF Computer Graphics Laboratory.

REFERENCES

Blum, M., Metcalf, P., Harrison, S. C., & Wiley, D. C. (1987) *J. Appl. Crystallogr. 20*, 235−242.

Brunger, A. T., Kuriyan, J., & Karplus, M. (1987) *Science 235*, 458−460.

Chaiet, L., & Wolf, F. J. (1964) *Arch. Biochem. Biophys. 106*, 1−5.

Chambers, J. L., & Stroud, R. M. (1979) *Acta Crystallogr. B35*, 1861−1874.
Climie, S., Ruiz-Perez, L., Gonzalez-Pacanowska, D., Prapunwattana, P., Cho, S.-W., Stroud, R., & Santi, D. V. (1990) *J. Biol. Chem. 265*, 18776−18779.
Costi, P. M., Liu, L., Finer-Moore, J. S., Stroud, R. M., & Santi, D. V. (1996) *Biochemistry* (in press).
Davies, D. R. (1990) *Annu. Rev. Biophys. Biophys. Chem. 19*, 189−215.
Derewenda, Z. S., Derewenda, U., & Kobos, P. M. (1994) *J. Mol. Biol. 241*, 83−93.
Ferrin, T. E., Huang, C. C., Jarvis, L. E., & Langridge, R. (1988) *J. Mol. Graphics 6*, 2−12.
Fersht, A. (1985) *Enzyme Structure and Mechanism*, pp 317−319, W. H. Freeman and Co., New York.
Finer-Moore, J., Fauman, E. B., Foster, P. G., Perry, K. M., Santi, D. V., & Stroud, R. M. (1993) *J. Mol. Biol. 232*, 1101−1116.
Finer-Moore, J. S., Fauman, E. B., Morse, R. J., Santi, D. V., & Stroud, R. M. (1996) *Protein Eng.* (in press).
Graves, K. L., Butler, M. M., & Hardy, L. W. (1992) *Biochemistry 31*, 10315−10321.
Hardy, L. W., & Nalivaika, E. (1992) *Proc. Natl. Acad. Sci. U.S.A. 89*, 9725−9729.
Hardy, L. W., Finer-Moore, J. S., Montfort, W. R., Jones, M. O., Santi, D. V., & Stroud, R. M. (1987) *Science 235*, 448−455.
Higashi, T. (1990) *J. Appl. Crystallogr. 23*, 253−257.
Jones, T. A. (1985) *Methods Enzymol. 115*, 157−171.
Kabsch, W. (1988) *J. Appl. Crystallogr. 21*, 916−924.
Kealey, J. T., & Santi, D. V. (1992) *Protein Expression Purif. 3*, 380−385.
Klimasauskas, S., & Roberts, R. J. (1995) *Nucleic Acids Res. 23*, 1388−1395.
Klimasauskas, S., Kumar, S., Roberts, R. J., & Cheng, X. (1994) *Cell 76*, 357−369.
Kraulis, P. J. (1991) *J. Appl. Crystallogr. 24*, 946−950.
Langsetmo, K., Fuchs, J. A., & Woodward, C. (1991) *Biochemistry 30*, 7603−7609.
Liu, L., & Santi, D. V. (1992) *Biochemistry 31*, 5100−5104.
Liu, L., & Santi, D. V. (1993a) *Biochemistry 32*, 9263−9267.
Liu, L., & Santi, D. V. (1993b) *Proc. Natl. Acad. Sci. U.S.A. 90*, 8604−8608.
Maley, G. F. (1978) *Methods Enzymol. 51*, 412−418.
Matthews, D. A., Villafranca, J. E., Janson, C. A., Smith, W. W., Welsh, K., & Freer, S. (1990) *J. Mol. Biol. 214*, 937−948.
Montfort, W. R., Perry, K. M., Fauman, E. B., Finer-Moore, J. S., Maley, G. F., Hardy, L., Maley, F., & Stroud, R. M. (1990) *Biochemistry 29*, 6964−6977.
Perry, K. M., Fauman, E. B., Finer-Moore, J. S., Montfort, W. R., Maley, G. F., Maley, F., & Stroud, R. M. (1990) *Proteins: Struct., Funct., Genet. 8*, 315−333.
Rastelli, G., Thomas, B., Kollman, P. A., & Santi, D. V. (1995) *J. Am. Chem. Soc. 117*, 7213−7227.
Reinisch, K. M., Chen, L., Verdine, G. L., & Lipscomb, W. N. (1995) *Cell 82*, 143−153.
Sack, J. S. (1988) *J. Mol. Graphics 6*, 224−225.
Sato, M., Yamamoto, M., Imada, K., Katsube, Y., Tanaka, N., & Higashi, T. (1992) *J. Appl. Crystallogr. 25*, 348−357.
Stroud, R. M., & Fauman, E. B. (1995) *Protein Sci. 4*, 2392−2404.
Wentworth, D. F., & Wolfenden, R. (1978) *Methods Enzymol. 51*, 401−407.

BI952751X